

This work has been submitted to the IEEE for possible publication. Copyright may be transferred without notice, after which this version may no longer be accessible.

Effective Overloaded Pilot Assignment with Pilot Decontamination for Cell-Free Systems

Noboru Osawa*, Fabian Göttsch[†], Issei Kanno*, Takeo Ohseki*,
Yoshiaki Amano*, Kosuke Yamazaki*, Giuseppe Caire[†]

*KDDI Research Inc., Saitama, Japan

[†]Technical University of Berlin, Germany

Emails: {nb-oosawa, is-kanno, ohseki, yo-amano, ko-yamazaki}@kddi-research.jp, {fabian.goettsch, caire}@tu-berlin.de

Abstract—The pilot contamination in cell-free massive multiple-input-multiple-output (CF-mMIMO) must be addressed for accommodating a large number of users. We have investigated a decontamination method called subspace projection (SP). The SP separates interference from co-pilot users by using the orthogonality of subspaces of each users' principal components. The SP based decontamination has a potential to further improve spectral efficiency (SE), which is limited by a non-overloaded pilot assignment (PA) rule where each radio unit (RU) does not assign the same pilot to different users. Motivated by this limitation, this paper introduces semi-overloaded and overloaded PA methods adjusted for the decontamination in order to improve the sum SE of CF systems. Numerical simulations show that the overloaded and semi-overloaded PA give higher SE than that of non-overloaded PA at a high user density scenario.

Index Terms—Cell-free massive MIMO, user-centric, pilot contamination, pilot assignment.

I. INTRODUCTION

A large number of works in wireless communication theory are dedicated to the joint processing of spatially distributed antennas. This idea can be traced back to the work of Wyner [1], and has been “re-marketed” several times under different names with slight nuances, such as coordinate multipoint (CoMP), cloud radio access network (CRAN), and currently, it is promoted as cell-free massive MIMO (CF-mMIMO). As the name implies, one of the purposes of CF-mMIMO is eliminating cell boundaries and the prevent user equipment's (UE's) performance degradation depending on their geographical positions.

The channel state information (CSI) acquisition with pilot signals at the infrastructure antenna side is important for taking advantage of CF-mMIMO's spatial multiplexing gain. In this paper, we focus on uplink (UL) channel estimation in a time division duplex (TDD) system. Thanks to TDD operations and channel reciprocity, these estimates can also be used for the downlink precoding [2]. Generally, the number of orthogonal pilots is limited to reduce overhead and keep the training phase within coherence time. Therefore, pilot reuse is inevitable to increase UEs to be accommodated, and it induces pilot contamination. In addition, CF-mMIMO system has no clear boundaries, it is hard to apply a cell-based pilot reuse restriction. Since pilot contamination degrades the accuracy of channel estimation, it is addressed to improve the system performance.

As one of the pilot decontamination methods, in [3], [4], we have investigated a subspace projection (SP) based channel

estimation, which uses receiver side discrete Fourier transform (DFT) processing. In this paper, channel subspace means the space on dominant signals of the MIMO channel covariance matrix which is observed by applying principal component analysis (PCA). Furthermore, assuming uniform linear arrays (ULAs) and uniform planar arrays (UPAs), the subspace of the covariance matrix is approximately diagonalized by DFT. Therefore, our proposed SP uses DFT to project signals into each user's subspace. If the antennas have correlation due to a limited scattering angular spread, each radio unit (RU) and UE link has an individual channel subspace. Thus, this projection extracts the subspace of the desired UE and eliminates the pilot contamination from the co-pilot UEs. We have shown that the effect of the pilot contamination can be reduced significantly with the SP, yielding a system performance close to the case of ideal CSI [3], where each RU has perfect knowledge of the channel vectors of its associated UEs.

The system model of CF in our previous works [3] is similar to Björnson and Sanguinetti's scalable CF system [5] where decentralized units (DUs) handles a finite number of user-centric clusters, and each cluster is formed by a finite number of RUs. In this CF system, we have not allowed each RU to assign the same pilot to different users, which we call non-overloaded pilot assignment (PA). However, the SP enhances RUs to estimate channels of co-pilot UEs under overloaded PA where RUs can assign the same pilot to multiple UEs. Adopting the overloaded PA leads to an increased number of associated RUs per UE, which could increase the spatial multiplexing gain per UE and improve spectral efficiency (SE).

Motivated by this, this paper investigates overloaded PA and semi-overloaded PA methods to improve the SE performance. The main difference between the overloaded and semi-overloaded PA is the formation process of user-centric clusters. The overloaded PA forms clusters in advance without considering the contamination, and then assign the pilots. On the other hand, the semi-overloaded PA has a restriction in the cluster formation phase that the method joins RUs into clusters of co-pilot UEs only when the subspaces of co-pilot UEs are orthogonal. In addition, the pilot assignment design of the overloaded PA has some variations, therefore we propose a specific implementation of overloaded PA by adjusting a graphic framework based PA studied by Zeng et al. [6] to our SP based decontamination.

The contributions of this work are summarized as follows.

- We propose a graphic framework-based PA adjusted for the SP as a specific implementation of overloaded PA.
- We investigate a semi-overloaded PA and corresponding cluster formation method for it. The benefit of semi-overloaded PA is a scalable implementation compared to the overloaded PA, since the overloaded PA requires network-wide metric calculation and information exchange.
- We compare the sum SE performance of the non-overloaded, semi-overloaded and overloaded PA, and reveal a region of parameters where the system achieves the largest sum SE.

II. SYSTEM MODEL

We consider a CF-mMIMO system with L RUs, each with M antennas, and K UEs. Both RUs and UEs are distributed on a squared region on the 2-dimensional plane. Here we assume that all clusters are already formed. The set $\mathcal{C}_k \subseteq [L] = \{1, 2, \dots, L\}$ denotes the cluster of RUs serving UE k and $\mathcal{U}_\ell \subseteq [K]$ denotes the set of UEs served by RU ℓ .¹ The RU-UE associations are described by a bipartite graph \mathcal{G} whose vertices are the RUs and UEs, respectively. The set of edges accounting for associated RU-UE pairs is denoted by \mathcal{E} , i.e., $\mathcal{G} = \mathcal{G}([L], [K], \mathcal{E})$. We also define $\mathcal{U}(\mathcal{C}_k) = \bigcup_{\ell \in \mathcal{C}_k} \mathcal{U}_\ell$ as the set of UEs served by at least one RU in \mathcal{C}_k .

In UL transmissions, the UEs transmit with the same energy per symbol E_s , and we define the system parameter

$$\text{SNR} = \frac{E_s}{N_0}, \quad (1)$$

where N_0 denotes noise power spectral density. The large-scale-fading-coefficient (LSFC) between RU ℓ and UE k is denoted by $\beta_{\ell,k}$ and includes pathloss, blocking effects and shadowing, respectively. By assuming isotropic antennas, the maximum beamforming gain averaged over the small scale fading is M , therefore the maximum SNR at the receiver of RU ℓ from UE k is $\beta_{\ell,k}MSNR$. This SNR is used as a criterion of cluster formation.

We consider orthogonal frequency-division multiplexing (OFDM) modulation and channels following the standard block-fading model [2], [7], [8], such that they are random but constant over coherence blocks of T signal dimensions in the time-frequency domain. The described methods are formulated for one resource block (RB), so the RB index is omitted for simplicity. We define channel matrices and its elements as follows. $\mathbb{H} \in \mathbb{C}^{LM \times K}$ denotes the overall channel matrix between all LM RU antennas and all K UE antennas on a given RB. Next, $\mathbf{h}_k \in \mathbb{C}^{LM \times 1}$ denotes k -th column of $\mathbb{H} \in \mathbb{C}^{LM \times K}$. In addition, $\mathbf{h}_{\ell,j} \in \mathbb{C}^{M \times 1}$ denotes the channel vector between RU ℓ and UE k . Finally, $\mathbb{H}(\mathcal{C}_k) \in \mathbb{C}^{LM \times K}$ denotes the partial cluster-centric matrix for a cluster \mathcal{C}_k , whose $M \times 1$ blocks of RU-UE pairs $(\ell, j) \in \mathcal{E}$ are equal to $\mathbf{h}_{\ell,j}$, and equal to $\mathbf{0}$ (the identically zero vector) otherwise. Then, we assume that the

individual channels between RUs and UEs follow the single ring local scattering model [9], then $\mathbf{h}_{\ell,j}$ is given by

$$\mathbf{h}_{\ell,k} = \sqrt{\frac{\beta_{\ell,k}M}{|\mathcal{S}_{\ell,k}|}} \mathbf{F}_{\ell,k} \boldsymbol{\nu}_{\ell,k}, \quad (2)$$

where $\mathcal{S}_{\ell,k} \subseteq \{0, \dots, M-1\}$ and $\boldsymbol{\nu}_{\ell,k}$ are the angular support set according to [9], an $|\mathcal{S}_{\ell,k}| \times 1$ i.i.d. Gaussian vector with components $\sim \mathcal{CN}(0, 1)$, respectively. The set $\mathcal{S}_{\ell,k}$ is constructed by the angular support $\Theta_{\ell,k} = [\theta_{\ell,k} - \Delta/2, \theta_{\ell,k} + \Delta/2]$ centered at angle $\theta_{\ell,k}$ of the LOS between RU ℓ and UE k , with angular spread Δ . We let \mathbf{F} denote $M \times M$ unitary DFT matrix with (m, n) -elements $f_{m,n} = \frac{e^{-j\frac{2\pi}{M}mn}}{\sqrt{M}}$, and using a Matlab-like notation, $\mathbf{F}_{\ell,k} \triangleq \mathbf{F}(:, \mathcal{S}_{\ell,k})$ denotes the tall unitary matrix obtained by selecting the columns of \mathbf{F} corresponding to the index set $\mathcal{S}_{\ell,k}$. If two users are located in the same Δ -wide angle with respect to a RU, their channel vectors will have identical subspace and therefore identical covariance matrix.

A. UL data transmission

We employ a local linear MMSE (LMMSE) with cluster-level combining as UL combining method. The details of local LMMSE are described in [3], where other methods such as cluster-level zero-forcing and local MRC are also discussed. Since the local LMMSE with cluster-level combining showed high performance with scalability in [3], we choose this scheme.

The received $LM \times 1$ symbol vector at the LM RU antennas in UL is given by

$$\mathbf{y}^{\text{ul}} = \sqrt{\text{SNR}} \mathbb{H} \mathbf{s}^{\text{ul}} + \mathbf{z}^{\text{ul}}, \quad (3)$$

where $\mathbf{s}^{\text{ul}} \in \mathbb{C}^{K \times 1}$ is the vector of information symbols transmitted by the UEs and \mathbf{z}^{ul} is an i.i.d. noise vector with components $\sim \mathcal{CN}(0, 1)$. We define received symbols vector of RU ℓ as $\mathbf{y}_\ell^{\text{ul}} \in \mathbb{C}^{LM \times 1}$, and receiver unit norm vector $\mathbf{v}_k \in \mathbb{C}^{LM \times 1}$ formed by $M \times 1$ blocks $\mathbf{v}_{\ell,k} : \ell = 1, \dots, L$, such that $\mathbf{v}_{\ell,k} = \mathbf{0}$ if $(\ell, k) \notin \mathcal{E}$. In the local LMMSE with cluster-level combining, each RU ℓ computes LMMSE local receiving vectors $\mathbf{v}_{\ell,k}$ for its UEs $k \in \mathcal{U}_\ell$ and combines received antenna symbols with $\mathbf{v}_{\ell,k}^H$, then cluster-level combining is applied with combining coefficient vector \mathbf{w}_k at each cluster \mathcal{C}_k . The LMMSE receiving vector $\mathbf{v}_{\ell,k}$ is given by

$$\mathbf{v}_{\ell,k} = \left(\sigma_\ell^2 \mathbf{I} + \text{SNR} \sum_{j \in \mathcal{U}_\ell} \mathbf{h}_{\ell,j} \mathbf{h}_{\ell,j}^H \right)^{-1} \mathbf{h}_{\ell,k}, \quad (4)$$

where σ_ℓ^2 denotes variance of external interference [10], given by

$$\sigma_\ell^2 = 1 + \text{SNR} \sum_{j \neq \mathcal{U}_\ell} \beta_{\ell,j}. \quad (5)$$

RU computes the local detector $r_{\ell,k}^{\text{ul}} = \mathbf{v}_{\ell,k}^H \mathbf{y}_\ell^{\text{ul}}$ for each $k \in \mathcal{U}_\ell$ and sends the symbols to the DUs for the cluster-level combining. Then the DU computes the cluster-level combined symbol as

$$r_k^{\text{ul}} = \sum_{\ell \in \mathcal{C}_k} w_{\ell,k} r_{\ell,k}^{\text{ul}}. \quad (6)$$

¹The set of integers from 1 to n is denoted by $[n]$.

The optimized combining weights vector $\mathbf{w}_k = \{w_{\ell,k} : \ell \in \mathcal{C}_k\}$, which maximizes the SINR [3], are given by

$$\mathbf{w}_k = \mathbf{\Gamma}_k^{-1} \mathbf{a}_k \in \mathbb{C}^{|\mathcal{C}_k| \times 1}, \quad (7)$$

$$\mathbf{a}_k = \{g_{\ell,k,k} : \ell \in \mathcal{C}_k\}, \quad (8)$$

$$g_{\ell,k,j} = \mathbf{v}_{\ell,k}^H \mathbf{h}_{\ell,j}, \quad (9)$$

$$\mathbf{\Gamma}_k = \mathbf{D}_k + \text{SNR} \mathbf{G}_k \mathbf{G}_k^H \in \mathbb{C}^{|\mathcal{C}_k| \times |\mathcal{C}_k|}, \quad (10)$$

$$\mathbf{D}_k = \text{diag} \{ \sigma_\ell^2 \|\mathbf{v}_{\ell,k}\|^2 : \ell \in \mathcal{C}_k \}, \quad (11)$$

where the matrix \mathbf{G}_k of dimension $|\mathcal{C}_k| \times (|\mathcal{U}(\mathcal{C}_k)| - 1)$ contains elements $g_{\ell,k,j}$ in position corresponding to RU ℓ and UE j (after a suitable index reordering) if $(\ell, j) \in \mathcal{E}$, and zero elsewhere. The overall receiving vector \mathbf{v}_k is formed by stacking the vectors $w_{\ell,k} \mathbf{v}_{\ell,k}$, i.e., $\mathbf{v}_k = [w_{1,k} \mathbf{v}_{1,k}^T, w_{2,k} \mathbf{v}_{2,k}^T, \dots, w_{L,k} \mathbf{v}_{L,k}^T]^T$.

B. UL SINR and SE

The resulting SINR for UE k 's UL symbol is given by

$$\text{SINR}_k^{\text{ul}} = \frac{|\mathbf{v}_k^H \mathbf{h}_k|^2}{\text{SNR}^{-1} + \sum_{j \neq k} |\mathbf{v}_k^H \mathbf{h}_j|^2}. \quad (12)$$

We use the optimistic ergodic achievable rate R_k^{ul} for performance evaluation, which is given by

$$R_k^{\text{ul}} = \mathbb{E} \left[\log(1 + \text{SINR}_k^{\text{ul}}) \right], \quad (13)$$

where the expectation is with respect to the small scale fading. Then, the UL spectral efficiency (SE) is calculated as

$$\text{SE}_k^{\text{ul}} = (1 - \tau_p/T) R_k^{\text{ul}}, \quad (14)$$

where T is the dimension of an RB and τ_p is the pilot dimension.

C. UL channel estimation

As a practical remark, we note that in 5GNR two types of UL pilots are specified, the demodulation reference signals (DMRS) and the sounding reference signals (SRS). In this work we assume that the instantaneous channel coefficients are estimated from DMRS pilots, and the subspace information is estimated by utilizing SRSs.²

The DMRS pilot received at RU ℓ is given by the $M \times \tau_p$ matrix as

$$\mathbf{Y}_\ell^{\text{DMRS}} = \sum_{i=1}^K \mathbf{h}_{\ell,i} \phi_{t_i}^H + \mathbf{Z}_\ell^{\text{DMRS}}, \quad (15)$$

where ϕ_{t_i} denotes the DMRS pilot vector of dimension τ_p used by UE i in the current RB, with total energy $\|\phi_{t_i}\|^2 = \tau_p \text{SNR}$. For each UE $k \in \mathcal{U}_\ell$, RU ℓ produces the *pilot matching* (PM) channel estimates

$$\begin{aligned} \hat{\mathbf{h}}_{\ell,k}^{\text{pm}} &= \frac{1}{\tau_p \text{SNR}} \mathbf{Y}_\ell^{\text{DMRS}} \phi_{t_k} \\ &= \mathbf{h}_{\ell,k} + \sum_{\substack{i:t_i=t_k \\ i \neq k}} \mathbf{h}_{\ell,i} + \tilde{\mathbf{z}}_{t_k,\ell}, \end{aligned} \quad (16)$$

where $\tilde{\mathbf{z}}_{t_k,\ell}$ has i.i.d. with components $\mathcal{CN}(0, \frac{1}{\tau_p \text{SNR}})$. Notice that the presence of UEs $i \neq k$ using the same DMRS pilot t_k yields pilot contamination.

Let us assume that the subspace information $\mathbf{F}_{\ell,k}$ of all $k \in \mathcal{U}_\ell$ is obtained from periodical SRS observation. We consider

²An estimation method of subspace information by utilizing SRSs are discussed in [10].

the SP based decontamination scheme for which the projected channel estimate is given by the orthogonal projection of $\hat{\mathbf{h}}_{\ell,k}^{\text{pm}}$ onto the subspace spanned by the columns of $\mathbf{F}_{\ell,k}$, i.e.,

$$\begin{aligned} \hat{\mathbf{h}}_{\ell,k}^{\text{sp}} &= \mathbf{F}_{\ell,k} \mathbf{F}_{\ell,k}^H \hat{\mathbf{h}}_{\ell,k}^{\text{pm}} \\ &= \mathbf{h}_{\ell,k} + \sum_{\substack{i:t_i=t_k \\ i \neq k}} \mathbf{F}_{\ell,k} \mathbf{F}_{\ell,k}^H \mathbf{h}_{\ell,i} + \mathbf{F}_{\ell,k} \mathbf{F}_{\ell,k}^H \tilde{\mathbf{z}}_{t_k,\ell}. \end{aligned} \quad (17)$$

The second term of the last equation corresponds to pilot contamination after the SP, which is a Gaussian vector with zero mean and its covariance matrix can be written as

$$\Sigma_{\ell,k}^{\text{co}} = \sum_{\substack{i:t_i=t_k \\ i \neq k}} \frac{\beta_{\ell,i} M}{|\mathcal{S}_{\ell,i}|} \mathbf{F}_{\ell,k} \mathbf{F}_{\ell,k}^H \mathbf{F}_{\ell,i} \mathbf{F}_{\ell,i}^H \mathbf{F}_{\ell,k} \mathbf{F}_{\ell,k}^H. \quad (18)$$

When $\mathbf{F}_{\ell,k}$ and $\mathbf{F}_{\ell,i}$ are nearly mutually orthogonal, i.e. $\mathbf{F}_{\ell,k}^H \mathbf{F}_{\ell,i} \approx \mathbf{0}$, the subspace projection is able to reduce the pilot contamination effect.

III. PILOT ASSIGNMENT AND CLUSTER FORMATION

Our previous work [3] applies joint DMRS assignment and cluster formation as non-overloaded PA. On the other hand, most of related works, which aimed to address contamination by strategic PA methods, implicitly adopted overloaded PA because non-overloaded PA has less freedom of assignment. In [11], a greedy PA algorithm was introduced as an early study in the CF literature. A pilot optimization with user throughput maximization is investigated in [12], where the maximization problem is solved by using an iterative scheme based on the Hungarian algorithm. In [13], user-group PA was proposed which assigns the same pilot to UEs who share less serving RUs. Furthermore, graphic framework based pilot assignment schemes are investigated in [6], [14].

As mentioned in Sec. 1, the SP can enhance overloaded PA, and it leads to improved SE. This section introduces non-overloaded, semi-overloaded and overloaded PA schemes with their cluster formation rules.

A. Non-overloaded pilot assignment

Let τ_p denotes the orthogonal DMRS dimension in the system. According to the non-overloaded PA, each RU assigns distinct pilots to all its associated UEs. When a UE k wishes to join the system, it selects its leading RU $\ell(k)$ as the one with the largest LSFC out of the set of RUs through some beacon signal or some other location-based mechanism. The RU $\ell(k)$ is imposed a condition that the RU has free DMRS pilots which have not yet been assigned by the RU to its served UEs. This is formulated as $\ell(k) = \arg \max_{\ell \in \mathcal{L}_f} \beta_{\ell,k}$, where \mathcal{L}_f denotes the set of RUs with free DMRS pilots. The leader RU selection also needs to satisfy the condition

$$\beta_{\ell,k} \geq \frac{\eta}{M \text{SNR}}, \quad (19)$$

where $\eta > 0$ is a suitable threshold determining how much above the noise floor the useful signal in the presence of maximum possible beamforming gain (equal to M) should be. If such RU is not available, then the UE is declared in outage.

The RU chooses a pilot with least interference for UE k . Let the RU ℓ acquire interference per pilot as statistics, k -th UE's pilot t_k is given by

$$t_k = \arg \min_{i \in \mathcal{T}_\ell} \sum_{j \in \mathcal{P}_i} \beta_{\ell,j}, \quad (20)$$

where \mathcal{T}_ℓ and \mathcal{P}_i denote a set of not assigned pilots at RU ℓ and a set of UEs with the same pilot index i , respectively. The set \mathcal{P}_i is updated as $\mathcal{P}_i = \mathcal{P}_i \cup k$ after assignment of t_k . The RU only knows the result of summation $\sum_{j \in \mathcal{P}_i} \beta_{\ell,j}$ as measured statistics.

Suppose that UE k finds its leader RU $\ell(k)$ and it is allocated the DMRS pilot with index $t_k \in [\tau_p]$. Then, the cluster \mathcal{C}_k is obtained sorting the RUs satisfying condition (19) and having pilot t_k still available in decreasing LSFC order, and adding them to the cluster until a maximum cluster size Q is reached, where Q is a design parameter imposed to limit the computational complexity of each cluster processor. As a result, for all UEs k not in outage, $1 \leq |\mathcal{C}_k| \leq Q$ and for all the RUs $\ell \in \mathcal{C}_k$, the corresponding LSFC satisfies (19). Furthermore, for all RUs ℓ we have $|\mathcal{U}_\ell| \leq \tau_p$.

B. Semi-overloaded pilot assignment based on subspace orthogonality

We introduce a semi-overloaded PA approach where each RU assigns the same pilot only to UEs with orthogonal subspaces. Let us assume that the RUs acquire subspace information of UEs within its coverage before the leader RU selection phase. At the leader RU selection phase, UEs firstly try to choose a RU with the largest LSFC as $\ell(k)$. If the RU $\ell(k)$ has free pilots, the RU selects a pilot based on eq. (20). On the other hand, when the RU has no free pilot, the RU tries to find a pilot which is orthogonal to other served UEs in the subspace. The pilot selection for UE k is formulated by using co-pilot UE set \mathcal{P}_i ($i \in [\tau_p]$) as

$$\zeta_{\ell,k,i} \triangleq \sum_{j \in (\mathcal{U}_\ell \cap \mathcal{P}_i \setminus k)} \|\mathbf{F}_{\ell,k} \mathbf{F}_{\ell,k}^H \mathbf{F}_{\ell,j}\|_F \beta_{\ell,j}, \quad (21)$$

$$\mathcal{A}_{\ell,k} \triangleq \{i | i \in [\tau_p], \zeta_{\ell,k,i} = 0\}, \quad (22)$$

$$t_k = \arg \min_{i \in \mathcal{A}_{\ell,k}} \sum_{j \in \mathcal{P}_i} \beta_{\ell,j}, \quad (23)$$

where $\zeta_{\ell,k,i}$ denotes the contamination quantity per pilot index i on the subspace of the channel between RU $\ell(k)$ and UE k , and the set $\mathcal{A}_{\ell,k}$ denotes the set of pilot indices with condition $\zeta_{\ell,k,i} = 0$. Note that this condition is too simple for practical use since this paper adopts a simple channel model. The threshold of $\zeta_{\ell,k,i}$ should be relaxed for a more practical channel model. The third equation (23) selects the least interfered pilot, where interference from unserved UEs are considered. If the RU ℓ cannot satisfy the above conditions, the UE approaches the next candidate RU, or UEs are declared in outage if no RU is available.

After all active UEs are connected to its leading RUs, user-centric clusters are formed. In the cluster formation of UE k , the cluster \mathcal{C}_k is obtained sorting the RUs satisfying condition (19) and (22) in decreasing LSFC order, and adding them to the cluster until a maximum cluster size Q is reached.

C. Overloaded pilot assignment

In the overloaded PA, user-centric clusters are formed before pilot allocation. Each UE k chooses up to Q RUs with condition $\beta_{\ell,k} > \frac{\eta}{M \text{SNR}}$. Then pilots are assigned to each UE by random pilot assignment (RPA) or strategic PA. Note that the following strategic PA is implemented by a network side controller such as a central unit (CU), while RPA can be applied locally.

Here we propose a strategic PA based on weighted graphic framework (WGF) based PA proposed in [6]. At first, we introduce WGF-based heuristic PA of [6] where subspace orthogonality is not considered. The WGF scheme consists of two main phases: the construction of a weighted pilot contamination graph and Max k-Cut PA. The aim of the Max k-Cut algorithm is finding the optimal τ_p co-pilot UEs sets $\{\mathcal{V}_1, \mathcal{V}_2, \dots, \mathcal{V}_{\tau_p}\}$ so that the potential contamination is minimum. However, implementation of the pure Max k-Cut algorithm has high complexity, thus [6] introduces a heuristic approximation of the Max k-Cut. The heuristic approach consists of the following steps, where each variable is explained later.

- 1) Assign τ_p arbitrarily chosen UEs to τ_p subsets, one in each subset. Temporal subsets are given as $\mathcal{V}_1 = \{\text{UE}_1\}, \dots, \mathcal{V}_{\tau_p} = \{\text{UE}_{\tau_p}\}$.
- 2) Select one remaining UE i , calculate a weight between each subset and UE i as $W_{i,q} = \sum_{j \in \mathcal{V}_q} \omega_{i,j}$, where $\omega_{i,j}$ denotes a weight between two UEs.
- 3) Assign the UE to a subset featuring minimized increased weight as $q^* = \arg \min_q W_{i,q}$ and update subset as $\mathcal{V}_{q^*} = \mathcal{V}_{q^*} \cup \text{UE}_i$.
- 4) Iteratively repeat step 2) and 3) until the remaining UEs are assigned.

Firstly, a potential pilot contamination $\omega_{k,k'}$ between k -th and k' -th UEs is defined as

$$\omega_{k,k'} = \left| \frac{\sum_{\ell \in \mathcal{C}_k} \beta_{\ell,k'}}{\sum_{\ell \in \mathcal{C}_k} \beta_{\ell,k}} \right|^2 + \left| \frac{\sum_{\ell \in \mathcal{C}_{k'}} \beta_{\ell,k}}{\sum_{\ell \in \mathcal{C}_{k'}} \beta_{\ell,k'}} \right|^2, \quad (24)$$

where the first term on the right-hand side corresponds to the amount of interference from the k' -th UE to the k -th cluster \mathcal{C}_k , and the second term corresponds to interference from the k -th UE to $\mathcal{C}_{k'}$. Secondly, a weight between subset \mathcal{V}_p and \mathcal{V}_q is defined as

$$W_{p,q} = \sum_{i \in \mathcal{V}_p, j \in \mathcal{V}_q} \omega_{i,j}. \quad (25)$$

This scheme tends to assign UEs with high potential interference into the different subsets, thus UEs with potentially high interference could be given orthogonal pilots.

For further enhancing the robustness to the contamination, we modify the WGF PA so that the potential interference after the SP process becomes small, by taking the subspace information into account in the WGF metric. The new metric can be calculated by substituting the operation of SP $\mathbf{F}_{\ell,k} \mathbf{F}_{\ell,k}^H$

TABLE I
SIMULATION PARAMETERS

Area size (A)	$2 \times 2 \text{ km}^2$
Number of UEs (K)	100–1200
Number of RUs and RU antennas ($\{L, M\}$)	$\{10, 40\}, \{25, 16\}, \{50, 8\}, \{100, 4\}$
Pilot dimension (τ_p)	10, 20, 30
Maximum cluster size (Q)	10
Cluster formation threshold (η)	1
Pathloss model	3GPP urban microcell channel [15] with 3.7 GHz carrier frequency
Bandwidth per UE	10 MHz
Transmit power per UE	20 dBm
Noise power spectral density	−174 dBm/Hz
Dimension of a RB (T)	200
Angular spread (Δ)	$\pi/8$

into (24) as

$$\begin{aligned}
\omega_{k,k'}^{\text{SP}} &= \left| \sum_{\ell \in C_k} \|\mathbf{F}_{\ell,k} \mathbf{F}_{\ell,k}^H \mathbf{F}_{\ell,k'}\|_F \beta_{\ell,k'} / \sum_{\ell \in C_k} \beta_{\ell,k} \right|^2 \\
&+ \left| \sum_{\ell \in C_{k'}} \|\mathbf{F}_{\ell,k'} \mathbf{F}_{\ell,k'}^H \mathbf{F}_{\ell,k}\|_F \beta_{\ell,k} / \sum_{\ell \in C_{k'}} \beta_{\ell,k'} \right|^2 \\
&= \left| \sum_{\ell \in C_k} \frac{|\mathcal{S}_{\ell,k} \cap \mathcal{S}_{\ell,k'}|}{|\mathcal{S}_{\ell,k}|} \beta_{\ell,k'} / \sum_{\ell \in C_k} \beta_{\ell,k} \right|^2 \\
&+ \left| \sum_{\ell \in C_{k'}} \frac{|\mathcal{S}_{\ell,k'} \cap \mathcal{S}_{\ell,k}|}{|\mathcal{S}_{\ell,k'}|} \beta_{\ell,k} / \sum_{\ell \in C_{k'}} \beta_{\ell,k'} \right|^2. \quad (26)
\end{aligned}$$

If the subspaces of UE k and k' are orthogonal, i.e. $|\mathcal{S}_{\ell,k} \cap \mathcal{S}_{\ell,k'}| = 0$, the potential interference after SP is 0 and $\omega_{k,k'}^{\text{SP}}$ reflects it. One point to consider in using (26) is that these expressions make use of the LSFCs of not associated RU-UE pairs, i.e., $\beta_{\ell,k'}$ for pairs (ℓ, k') such that $\ell \notin C_{k'}$. Since RU ℓ is not part of the cluster serving user k' , such LSFCs may be difficult to be estimated and may not be available. On the other hand, if RU ℓ is not part of $C_{k'}$ it is likely that $\beta_{\ell,k'}$ is very small (otherwise the RU would be part of the cluster). Motivated by this, we introduce a partial LSFC-based WGF metric where only the LSFCs of associated UE-RU pairs are available, i.e.,

$$\begin{aligned}
\bar{\omega}_{k,k'}^{\text{SP}} &= \left| \sum_{\ell \in C_k \cap C_{k'}} \frac{|\mathcal{S}_{\ell,k} \cap \mathcal{S}_{\ell,k'}|}{|\mathcal{S}_{\ell,k}|} \beta_{\ell,k'} / \sum_{\ell \in C_k} \beta_{\ell,k} \right|^2 \\
&+ \left| \sum_{\ell \in C_{k'} \cap C_k} \frac{|\mathcal{S}_{\ell,k'} \cap \mathcal{S}_{\ell,k}|}{|\mathcal{S}_{\ell,k'}|} \beta_{\ell,k} / \sum_{\ell \in C_{k'}} \beta_{\ell,k'} \right|^2. \quad (27)
\end{aligned}$$

We substitute this partial LSFC-based metric into (25) for numerical simulations.

IV. SIMULATION RESULTS

Table I shows the basic parameter specifications of computer simulations. We consider a square coverage area of $A = 2 \times 2 \text{ km}^2$ with a torus topology by using the wrapped around technique to avoid boundary effects. LSFCs are given according to the 3GPP urban microcell street canyon pathloss model from [15, Table 7.4.1-1], which differentiates between UEs in LOS

TABLE II
THE LARGEST SUM SE WITH PARAMETERS

PA scheme	Sum SE [bit/s/Hz]	K	L	M	τ_p
Non-overloaded PA with PM	738	800	100	4	20
Non-overloaded PA with SP	770	800	100	4	20
Semi-overloaded PA with SP	866	600	25	16	30
Overloaded RPA with SP	740	400	50	8	30
Overloaded WGF-PA with SP	841	600	25	16	30

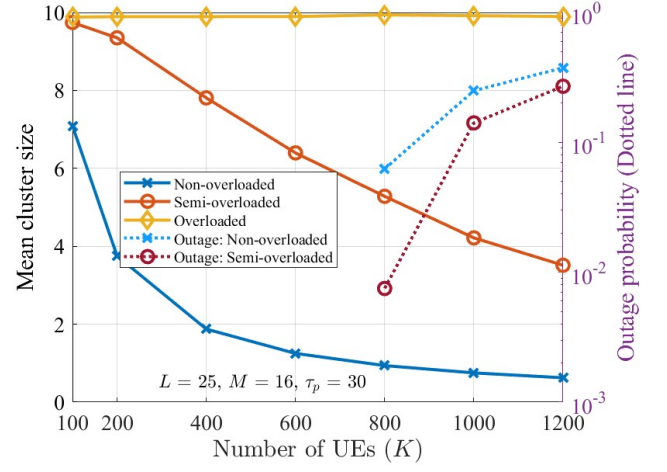


Fig. 1. Mean cluster size with outage probability vs. K .

and NLOS. The total number of receiving antenna is fixed as $LM = 400$. For each set of parameters we generated 40 independent layouts, and small scale fading coefficients are varied 30 times at each layouts. RUs and UEs are randomly distributed in each setup, and the sum SE is given by sum of SE_k^{ul} , and then averaging it with respect to the different layout.

Table II shows the largest sum SE and parameters L, M, K, τ_p at that setup. Firstly, we confirmed that $\tau_p = 30$ outperforms the result of $\tau_p \leq 20$ for the overloaded and the semi-overloaded PA even taking into account the overhead in eq. (14), while $\tau_p = 20$ is the best for the non-overloaded PA. Comparing each PA and channel estimation method, the semi-overloaded PA with SP achieves the highest sum SE. Then we focus on the setup $\tau_p = 30, L = 25, M = 16$ to analyze the behavior around the largest sum SE.

Fig. 1 shows mean cluster size with outage probability vs. K , and Fig. 2 illustrates the sum SE vs. K . Note that outage occurs in the region of more than 800 UEs for the semi-overloaded and the non-overloaded PA. From Fig. 1, the cluster size with overloaded PA becomes $Q \geq 9$ for most of UEs. From this observation, if there is no limitation on cluster formation, every UE can find RUs over Q with enough gain in this distribution and transmit power, then Q RUs join the cluster in order of gain. The cluster size of the non-overloaded PA

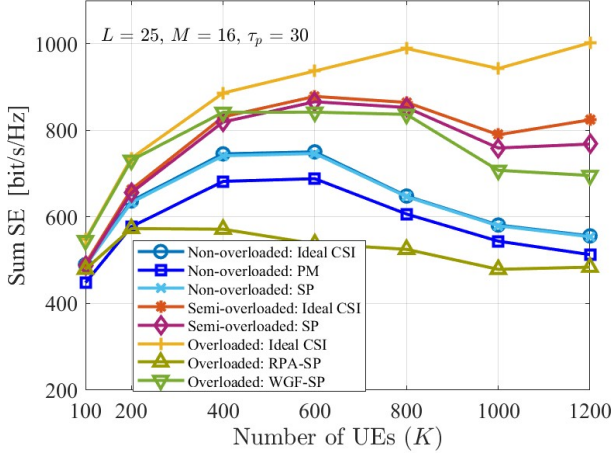


Fig. 2. Sum SE vs. K .

scheme is significantly reduced by the increase of K , while that of the semi-overloaded PA scheme decreases more gradual. If channel estimation has no error, UEs with larger clusters can be given higher SE by obtaining more spatial diversity. Thus, the overloaded and the semi-overloaded cluster formation have the potential to outperform the non-overloaded in terms of SE.

Then let us focus on Fig. 2 where Ideal CSI lines indicate no channel estimation error. The SE degradation factor can be divided into two: channel estimation error due to the contamination, and spatial multiplexing limit due to the increase of UEs. The fact that the sum SE saturates in the ideal CSI case indicates the latter factor.

For the non-overloaded PA, the PM channel estimation degrades from ideal CSI even for the smallest K . On the other hand, the SP achieves the same sum SE as the ideal case, which means that the SP effectively eliminates the contamination. For the overloaded PA, the performance of RPA significantly degrades from its upper bound (Ideal CSI) as K increases, as randomly assigned pilots generate many co-pilot UEs within the same subspace. The WGF-based PA also degrades from the ideal case, however, it achieves the highest sum SE at $K \leq 400$ among all PA methods. At last, for the semi-overloaded PA, it slightly outperforms the overloaded PA at $K \geq 600$ and achieves the highest sum SE at $K = 600$. In addition, the gap between the SP and the ideal CSI stays very small, thus the semi-overloaded PA seems to work as we expected. In the region of $K \geq 800$, the sum SE saturates and slightly degrades, which can be considered the effect of increased outage as seen in Fig. 1.

The overloaded WGF-based PA has the highest sum SE at certain UE density ($K \leq 400$), where the per UE SE (sum SE/ K) becomes the best, but the challenge of implementation remains due to the unscalable PA assignment. Thus the approximated implementation for scalability is desired for practical deployment. On the other hand, the semi-overloaded PA achieves a competitive sum SE at $K = 400$ with a relaxed PA procedure.

V. CONCLUSIONS

This paper has investigated the semi-overloaded and overloaded PA with the cluster formation methods that outperform the non-overloaded PA in CF-mMIMO systems. The overloaded WGF-based PA achieved the highest sum SE in the region of certain UE density ($K \leq 400$), while it is challenging for practical implementation due to the unscalable metric calculation and information exchange. The semi-overloaded PA, which only overloads UEs with orthogonal subspaces, achieves the highest sum SE in the region of $K \geq 600$. Furthermore, it also achieves a competitive sum SE at $K \geq 400$ with more relaxed PA procedure.

REFERENCES

- [1] A. D. Wyner, "Shannon-theoretic approach to a gaussian cellular multiple-access channel," *IEEE Trans. on Inform. Theory*, vol. 40, no. 6, pp. 1713–1727, 1994.
- [2] T. L. Marzetta, "Noncooperative cellular wireless with unlimited numbers of base station antennas," *IEEE Trans. on Wireless Comm.*, vol. 9, no. 11, pp. 3590–3600, 2010.
- [3] F. Göttsch, N. Osawa, T. Ohseki, K. Yamazaki, and G. Caire, "The impact of subspace-based pilot decontamination in user-centric scalable cell-free wireless networks," in *2021 IEEE 22nd International Workshop on Signal Processing Advances in Wireless Communications (SPAWC)*, 2021, pp. 406–410.
- [4] F. Göttsch, N. Osawa, T. Ohseki, K. Yamazaki, and G. Caire, "Uplink-downlink duality and precoding strategies with partial CSI in cell-free wireless networks," *CoRR*, vol. abs/2201.04922, 2022. [Online]. Available: <https://arxiv.org/abs/2201.04922>
- [5] E. Björnson and L. Sanguinetti, "Scalable cell-free massive mimo systems," *IEEE Trans. on Comm.*, vol. 68, no. 7, pp. 4247–4261, 2020.
- [6] W. Zeng, Y. He, B. Li, and S. Wang, "Pilot assignment for cell free massive mimo systems using a weighted graphic framework," *IEEE Transactions on Vehicular Technology*, vol. 70, no. 6, pp. 6190–6194, 2021.
- [7] Ö. T. Demir, E. Björnson, L. Sanguinetti *et al.*, "Foundations of User-Centric Cell-Free Massive MIMO," *Foundations and Trends® in Signal Processing*, vol. 14, no. 3-4, pp. 162–472, 2021.
- [8] E. Björnson and L. Sanguinetti, "Scalable cell-free massive mimo systems," *IEEE Trans. on Comm.*, vol. 68, no. 7, pp. 4247–4261, 2020.
- [9] A. Adhikary, J. Nam, J.-Y. Ahn, and G. Caire, "Joint Spatial Division and Multiplexing—The Large-Scale Array Regime," *IEEE Trans. on Inform. Theory*, vol. 59, no. 10, pp. 6441–6463, 2013.
- [10] F. Göttsch, N. Osawa, T. Ohseki, K. Yamazaki, and G. Caire, "Subspace-based pilot decontamination in user-centric scalable cell-free wireless networks," 2022. [Online]. Available: <https://arxiv.org/abs/2203.00714>
- [11] H. Q. Ngo, A. Ashikhmin, H. Yang, E. G. Larsson, and T. L. Marzetta, "Cell-free massive mimo versus small cells," *IEEE Transactions on Wireless Communications*, vol. 16, no. 3, pp. 1834–1850, 2017.
- [12] S. Buzzi, C. D'Andrea, M. Fresia, Y.-P. Zhang, and S. Feng, "Pilot assignment in cell-free massive mimo based on the hungarian algorithm," *IEEE Wireless Communications Letters*, vol. 10, no. 1, pp. 34–37, 2021.
- [13] S. Chen, J. Zhang, E. Björnson, J. Zhang, and B. Ai, "Structured massive access for scalable cell-free massive mimo systems," *IEEE Journal on Selected Areas in Communications*, vol. 39, no. 4, pp. 1086–1100, 2021.
- [14] W. H. Hmida, V. Meghdadi, A. Bouallegue, and J.-P. Cances, "Graph coloring based pilot reuse among interfering users in cell-free massive mimo," in *2020 IEEE International Conference on Communications Workshops (ICC Workshops)*, 2020, pp. 1–6.
- [15] 3GPP, "Study on channel model for frequencies from 0.5 to 100 GHz (Release 16)," 3GPP Technical Specification 38.901, 12 2019, Version 16.1.0.